Proc. Natl. Acad. Sci. USA
Vol. 93, pp. 4057–4062, April 1996
Biochemistry

DNA transport by a type II topoisomerase: Direct evidence for a two-gate mechanism

(protein engineering/disulfide crosslinking/enzyme mechanism/DNA topology)

JOAQUIM ROCA*†, JAMES M. BERGER*†‡, STEPHEN C. HARRISON§, AND JAMES C. WANG†

†Department of Molecular and Cellular Biology and §Howard Hughes Medical Institute, Harvard University, 7 Divinity Avenue, Cambridge, MA 02138

Contributed by James C. Wang, December 27, 1995

ABSTRACT **Recent biochemical and crystallographic results suggest that a type II DNA topoisomerase acts as an ATP-modulated clamp with two sets of jaws at opposite ends: a DNA-bound enzyme can admit a second DNA through one set of jaws; upon binding ATP, this DNA is passed through an enzyme-mediated opening in the first DNA and expelled from the enzyme through the other set of jaws. Experiments based on the introduction of reversible disulfide links across one dimer interface of yeast DNA topoisomerase II have confirmed this mechanism. The second DNA is found to enter the enzyme through the gate formed by the N-terminal parts of the enzyme and leave it through the gate close to the C termini.**

Type II DNA topoisomerases catalyze the ATP-dependent transport of one DNA double helix through another (1–3). All type II enzymes are structurally and evolutionarily related (4–10), and they participate in a number of cellular processes including chromosomal condensation and segregation (11). The enzymes are dimeric, and each half is composed of one, two, or three polypeptides, depending on the source of the enzyme. In the absence of nucleotides, the two halves contact each other primarily in a region located within the A subunit of bacterial gyrase or the gene *52* protein of the phage enzymes; in the case of the single subunit eukaryotic DNA topoisomerase II, this region is present near the C-terminal part of the polypeptide. ATP and its analogs can bind to a free or DNA-bound enzyme and induce the formation of additional contacts between the two halves. In solution, the binding of the β,γ-imido analog of ATP [adenosine 5′-[β,γ-imido]triphosphate (AMPPNP)] promotes dimerization of the N-terminal half of bacterial gyrase B subunit containing the ATPase site (12). The crystal structure of the same GyrB fragment with one bound AMPPNP per polypeptide also shows a dimer that is held together by a 14-residue N-terminal arm of one protomer and the core domain of the other protomer (13). Binding of AMPPNP or the γ-thio analog adenosine 5′-[γ-thio]triphosphate to yeast DNA topoisomerase II was shown to convert it from a form that can bind DNA of any topological form to one that binds only linear DNA (14). These results led to a model in which the enzyme acts as an ATP-modulated clamp: in the absence of ATP the two halves of the clamp are held together by dimer contacts near the C terminus of each polypeptide, and ATP binding leads to dimerization of the N-terminal domains to close the N-terminal entrance or the "N-gate" of the protein (14). In this model, the enzyme assumes an annular shape in its ATP-bound form, with a hole large enough to thread a linear DNA but not a double-stranded DNA loop through it. Catenation experiments between two sequentially added DNA rings, under processive conditions such that a second DNA ring could not displace a DNA ring already bound to the enzyme, showed that the first DNA bound was the one bearing the DNA gate—that is, the site of transient breakage by the enzyme. This DNA segment has been termed the gate segment or "G-segment" (14). Catenane formation was observed only when the second ring was added before the closure of the clamp mediated by AMPPNP binding, and thus the DNA segment being transported, which has been termed the "T-segment," appears to enter the interior of the enzyme through the N-gate. Presumably, when ATP binding triggers the closure of the N-gate, the T-segment is driven through the DNA gate in the G-segment (14).

How does the T-segment exit the enzyme after its entrance through the N-gate and passage through the G-segment? Two types of models were proposed. In the "two-gate model," the T-segment leaves the enzyme through a second gate on the opposite side of the entrance gate (15, 16). In the "one-gate model," the T-segment is kept in the interior of the enzyme after crossing the G-segment and is expelled from the enzyme when the N-gate reopens after ATP hydrolysis (17). The one-gate mechanism side steps the seemingly difficult feat of keeping the two halves of the enzyme from coming apart while passing a DNA through the entire dimer interface of the protein. It requires, however, that at least a portion of the rejoined G-segment be dissociated from the DNA binding surface of the enzyme before the exit of the T-segment—otherwise the exiting T-segment would have to pass back through the G-segment with no net topological change in the DNA rings containing these segments.

Recent experiments showed that the binding of AMPPNP to a yeast DNA topoisomerase II bound to a singly linked catenane led to efficient decatenation (18, 19). Furthermore, in such a single-step decatenation, the DNA ring containing the G-segment remained associated with the enzyme in its closed-clamp conformation, but the DNA ring containing the T-segment was found to be free in solution (18). Because the N-gate does not reopen after its closure by AMPPNP binding, the failure to find the transported DNA ring inside the closed enzyme clamp argues in favor of the two-gate model: that is, the DNA ring containing the T-segment, after its transport through the G-segment, exits the enzyme through the dimer interface in the C-terminal portion of the enzyme (18). This dimer interface will be referred to as the putative "C-gate" of the enzyme.

The experiments described above do not rule out, however, a scheme in which the T-segment enters and leaves the enzyme through the N-gate before the complete closure of this gate by AMPPNP binding. The recent determination of the three-dimensional crystal structure of a 92-kDa fragment of yeast DNA topoisomerase II (20) provides an opportunity to test the two models rigorously. This fragment, which lacks the first 409 residues of the functional enzyme (the ATPase domain), is a dimer in solution as well as in the crystal. The structure provides detailed three-dimensional information on the dimer

The publication costs of this article were defrayed in part by page charge payment. This article must therefore be hereby marked "*advertisement*" in accordance with 18 U.S.C. §1734 solely to indicate this fact.

Abbreviation: AMPPNP, adenosine 5′-[β,γ-imido]triphosphate.

*J.R. and J.M.B. contributed equally to this work.

‡Present address: The Whitehead Institute, Massachusetts Institute of Technology, Cambridge, MA 02139.

interface constituting the presumptive C-gate. By inspecting this interface, with computer graphics, disulfide links across the C-gate of a functional enzyme were designed. We report here studies with a mutant enzyme in which Asn-1043 and Lys-1127 were replaced by Cys. The formation of a pair of disulfide links across the C-terminal dimer interface in the mutant enzyme and the disruption of these links by treatment with 2-mercaptoethanol were used to show that the DNA segment transported by the yeast topoisomerase indeed passes through the entire interface between the two enzyme halves.

MATERIALS AND METHODS

Materials. Singly linked DNA catenane containing a supercoiled and a nicked DNA ring was prepared from pKS5 by using γδ resolvase (21), followed by treatment with *Bam*HI restriction endonuclease in the presence of excess ethidium (18). Oligodeoxynucleotide-directed codon replacements in a plasmid-borne *Saccharomyces cerevisiae TOP2* gene were carried out by the use of a commercial kit (Clontech). DNA samples from individual colonies were prepared, and their nucleotide sequences in the mutated regions were determined to verify the intended codon changes. Restriction fragments containing the correct Cys substitutions were used to replace the corresponding fragments in a yeast DNA topoisomerase II overexpression plasmid YEpTOP2PGAL1 (22). Growth, induction of the cloned gene by galactose addition, and cell disruption were done as described (23).

Among the four mutant enzymes, formation of disulfide crosslinks between two enzyme halves was evident only in the

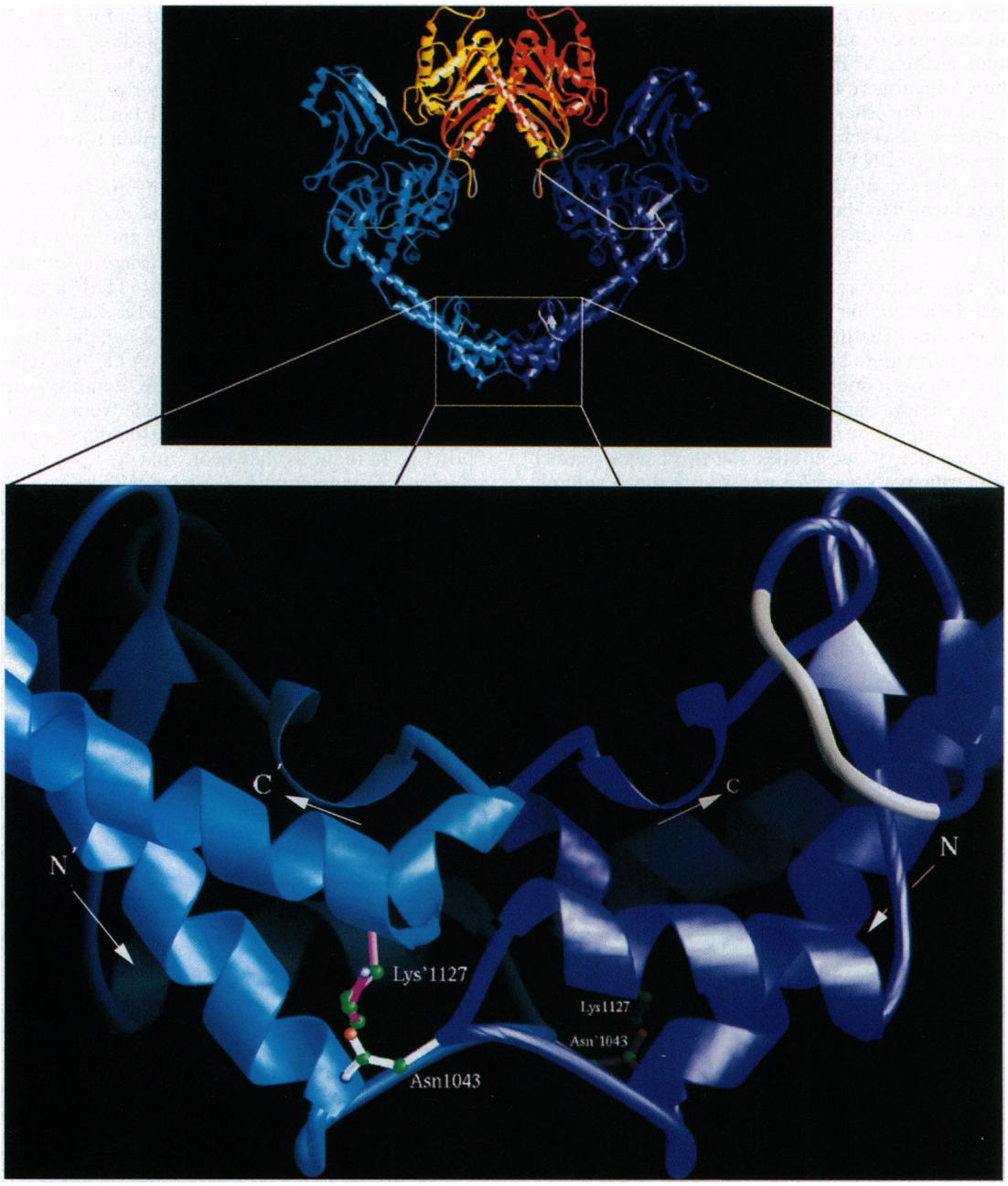

FIG. 1. (*Upper*) Ribbons model (25) of the crystal structure of the 92-kDa yeast DNA topoisomerase II fragment containing amino acid residues 410–1202 (20). The orange and purple sections of one protomer correspond to the C-terminal half of the B subunit and the N-terminal two-thirds of the A subunit of bacterial DNA gyrase, respectively; the corresponding sections in the other protomer are yellow and blue, respectively. (*Lower*) The portion of the structure containing the putative C-gate is enlarged. Lys-1127 and Asn-1043 are represented by stick-and-ball models. For clarity, a prime is used to designate residues in the left protomer. The arrows indicate the N- to C-terminal directions of the pair of antiparallel α-helices that extend from the core structure of each protomer to the dimer interface.

case of the N1043C–K1127C protein, in which the designated Asn and Lys were replaced by Cys; SDS/polyacrylamide gel electrophoresis of extracts of cells overexpressing the protein showed that its mobility was much reduced upon incubation of the freshly prepared extracts with oxidized glutathione. The N1043C–K1127C mutant was, therefore, selected for purification of milligram quantities of the enzyme by phosphocellulose and Q-Sepharose column chromatography (20). As a control, wild-type yeast DNA topoisomerase II was purified by the same procedure. Sulfhydryl reagents were omitted in all buffers.

Computer Modeling and Other Methods. Computer modeling of Cys substitutions was done on a Silicon Graphics Indigo2 station. By using the program O (24), the crystal structure of the 92-kDa yeast DNA topoisomerase II fragment was first inspected for pairs of residues across the dimer interface in which the side-chain C_β positions within a pair are 4–5 Å apart; Cys residues were then placed at the positions of these residues, and a pair of Cys residues were considered candidates for disulfide formation if their sulfur atoms are 2–3 Å apart and if the side-chain rotamers in the models are consistent with conformations of known disulfides.

One-step decatenation by wild-type or Cys-substituted yeast DNA topoisomerase II and analysis of the reaction products by DNA retention on a glass-fiber filter were done as described (14, 18). Isolation of individual DNA topoisomers and analysis of linking number changes of a topoisomer by wild-type or Cys-substituted enzyme were done as described (19).

RESULTS

Structure-Based Design of Disulfide Links Across the C-Terminal Dimer Interface of Yeast DNA Topoisomerase II. Fig. 1 shows the recently determined structure of the 92-kDa yeast DNA topoisomerase II fragment with an enlargement of the C-terminal dimerization domain, which is the major dimer interface between the two crescent-shaped monomers (20). Inspection of this interface by computer graphics led to the selection of four candidate pairs of residues for replacement by Cys residues and crosslinking of the two enzyme halves by disulfide bond formation. With the exception of Arg-1121, which could be mutated to Cys-1121 for disulfide bond formation with its dimer-related symmetry mate, the other three pairs of residues, Leu-1118–Trp-1123, Asn-1043–Lys-1127, and Ile-1035–Thr-1042, required double mutations in each polypeptide for the formation of two symmetry-related disulfide links across the dimer interface.

Among the four candidates, the N1043C–K1127C protein was found to form interprotomer disulfide links readily. When freshly prepared cell extracts overexpressing the mutant protein were analyzed by SDS/polyacrylamide gel electrophoresis in the absence of sulfhydryl reagent, the mobility of the mutant protein was that expected of a 170-kDa polypeptide (Fig. 2, lane 2). Its mobility was much reduced, however, after its purification and storage or upon treatment of cell extracts with oxidized glutathione (Fig. 2, lanes 3 and 4). The large reduction in mobility is consistent with formation of two disulfide links; the molecular mass would double, and the presence of 83 residues in each chain between the pair of disulfide links would result in the formation of a 166-residue bubble in the denatured dimer, which would further reduce the gel electrophoretic mobility.

Fig. 3 shows that both the crosslinked and uncrosslinked mutant enzyme cleave DNA efficiently in the presence of etoposide, a drug known to stabilize the DNA–protein covalent intermediate (26). In each case, treatment of the cleavage products with SDS and proteinase K revealed the formation of a prominent linear DNA band when the molar ratio of enzyme to DNA was less than 1 (Fig. 3, lanes 2 and 4). Cleavage of a DNA ring by the crosslinked mutant enzyme also provided a confirmation of the formation of interprotomer disulfide links in the mutant enzyme. When proteinase K treatment was

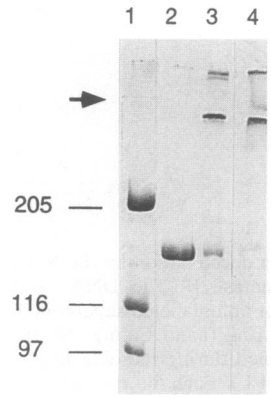

FIG. 2. SDS/polyacrylamide gel electrophoresis of the N1043C–K1127C mutant yeast DNA topoisomerase II. Lane 1 contained a mixture of marker proteins with their molecular masses (in kDa) indicated to the left. Each of the samples analyzed in lanes 2–4 contained ≈4 μg of the purified protein in 50 mM Tris acetate, pH 7.5/100 mM potassium acetate/5 mM magnesium acetate/0.5 mM ATP/2 μg of plasmid DNA/10% (vol/vol) glycerol. For the sample in lane 2, 2-mercaptoethanol was added to the mixture to a final concentration of 2 mM and the mixture was incubated at 30°C for 1 h, SDS was then added to 1%, and the mixture was heated at 95°C for 2 min before loading onto the gel. For the samples analyzed in lanes 3 and 4, 2-mercaptoethanol was omitted from the incubation mixture, the sample in lane 3 was treated with SDS without incubation at 30°C, and the sample in lane 4 was incubated for 1 h at 30°C before the addition of SDS. The running gel was 8% polyacrylamide (acrylamide/*N*,*N*′-methylenebisacrylamide ratio = 29:1); the boundary between the stacking and running gel is marked by an arrow. The gel was fixed, stained with Coomassie blue, dried, and photographed over a light box.

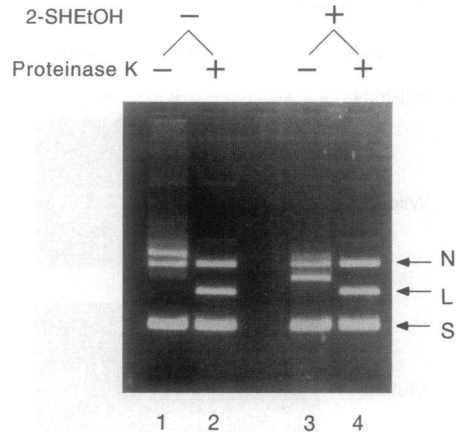

FIG. 3. Formation of covalent adduct between plasmid DNA and the N1043C–K1127C mutant yeast DNA topoisomerase in the presence and absence of 2-mercaptoethanol. The reaction mixture contained ≈2 pmol of a 3-kb plasmid DNA and 2 pmol of purified mutant enzyme in 100 μl of reaction buffer containing 50 mM Tris·HCl (pH 8), 150 mM KCl, 10 mM $MgCl_2$, 1 mM ATP, etoposide (VP-16; 100 μg/ml), and bovine serum albumin (100 μg/ml). After 10 min at 30°C, 10 μl of 10% (wt/vol) SDS was added to effect DNA cleavage and DNA–enzyme covalent adduct formation. The reaction mixture was then divided into four equal portions, and 2-mercaptoethanol and proteinase K were added to final concentrations of 7 mM and 100 μg/ml, respectively, in samples specified by the plus sign above the lanes, and all samples were incubated at 60°C for 30 min before loading on a 1% agarose gel. Electrophoresis was 2 h at 100 V in a buffer containing 50 mM Tris borate, 1 mM EDTA, ethidium bromide (0.5 μg/ml), and 0.1% SDS. The gel slab was photographed over a UV light box. The positions of nicked, linear, and supercoiled 3-kb DNA are marked by N, L, and S, respectively. The nature of the other bands in lanes 1 and 3 is explained in the text.

omitted, the cleavage product of the uncrosslinked enzyme migrated faster than nicked circular DNA but slower than linear DNA, because of the presence of protein moieties at the ends of the linearized DNA (Fig. 3, lane 3). However, the cleavage product of the crosslinked enzyme migrated more slowly than nicked circular DNA under the same condition (Fig. 3, lane 1), indicating that cleavage of a supercoiled DNA ring by a crosslinked enzyme yields a ring-shaped DNA–protein complex in which the two ends of the cleaved DNA are bridged by a pair of denatured disulfide-linked polypeptides.

Disulfide Links Across the C-Terminal Dimer Interface of Yeast DNA Topoisomerase II Impede Its Relaxation of Supercoiled DNA. As shown in Fig. 4, no relaxation activity was detectable in the absence of ATP (lane 1), demonstrating that the preparations were free of contaminating type I DNA topoisomerase activity. For the wild-type enzyme, the presence or absence of 2-mercaptoethanol had little effect on the reaction in medium containing 50 or 150 mM KCl (Fig. 4 *Upper*). For the mutant enzyme with specific disulfide links, the activity was significantly lower than that of the wild-type enzyme (compare Fig. 4 *Lower*, lanes 2 and 4, and *Upper*, lanes 2 and 4). Treatment of the crosslinked mutant enzyme with 2-mercaptoethanol increased its activity to that of the wild-type enzyme (compare Fig. 4 *Lower*, lanes 3 and 5, and *Upper*, lanes 3 and 5). These results indicate that the relaxation activity of the disulfide-crosslinked mutant enzyme was significantly diminished. Inspection of Fig. 4 *Lower*, lanes 2 and 4, reveals the presence of a linear DNA species in samples containing the crosslinked enzyme, suggesting that the formation of the specific disulfide links across the C-terminal dimer interface may favor DNA cleavage by the enzyme.

Crosslinking of Yeast Topoisomerase II Across Its C-Terminal Dimer Interface Prevents the Exit of the Transport DNA Ring from the Enzyme. Crosslinking of the C-terminal dimer interface of yeast DNA topoisomerase II allows a direct test of the two-gate model. The model predicts that in a one-step decatenation by the binding of AMPPNP to a crosslinked enzyme, the DNA ring containing the T-segment would not be able to exit through the C-gate and would remain topologically linked to the annular enzyme. The results of such an experiment are shown in Fig. 5. The catenane used contained a supercoiled DNA ring singly linked to a radiolabeled nicked DNA ring. The DNA was mixed with crosslinked N1043C–K1127C mutant enzyme at a molar ratio of about 1 and preincubated either in the presence of 2-mercaptoethanol to reduce the disulfide links or in the absence of the sulfhydryl reagent. AMPPNP was then added to each sample to effect the closure of the DNA-bound protein clamp and decatenation. After the addition of AMPPNP, NaCl was added to a final concentration of 1 M, and the mixture was filtered through a glass-fiber filter. Protein-free DNA recovered from the filtrate and protein-associated DNA recovered from the filter were analyzed by agarose gel electrophoresis. As shown (14, 18, 19), in the absence of the topoisomerase retention of DNA on the filter was insignificant; essentially all input DNA appeared in the filtrate fraction (Fig. 5, lane 1) and little DNA was recovered from the filter (Fig. 5, lane 2). Some linear DNA was formed during radiolabeling of the DNA catenane by nick translation (band L). For the enzyme–DNA mixture preincubated with 2-mercaptoethanol to reduce the interprotomer disulfide crosslinks in the mutant enzyme, the result was identical to those previously obtained with wild-type yeast DNA topoisomerase II (18, 19). Upon AMPPNP binding, the input catenane was efficiently decatenated by the enzyme bound to the supercoiled member of the dimeric catenane, and the nicked DNA ring containing the T-segment (band N) was found in the protein-free fraction after its transport through the G-segment in the supercoiled DNA (Fig. 5, lanes 3 and 4).

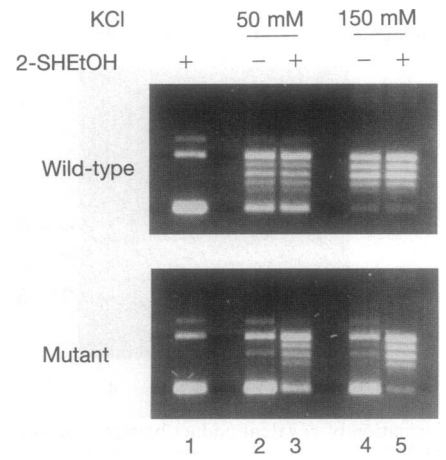

FIG. 4. Relaxation of negatively supercoiled DNA by wild-type yeast DNA topoisomerase II (*Upper*) and its N1043C–K1127C derivative (*Lower*). Each 50-μl reaction mixture contained 50 mM Tris·HCl (pH 8), 50 or 150 mM KCl as specified above the lanes, 10 mM $MgCl_2$, bovine serum albumin (100 μg/ml), 1 pmol of the wild-type or mutant topoisomerase, 1 pmol of supercoiled 3-kb plasmid DNA, and 7 mM 2-mercaptoethanol if indicated by a plus sign above the lane. The sample in lane 1 contained no ATP. In samples analyzed in the other lanes, ATP was added to 1 mM; after 1 min at 30°C, relaxation of supercoiled DNA by the topoisomerase was terminated by the addition of SDS to 1%. All samples were deproteinized by incubation with proteinase K (100 μg/ml) for 30 min at 60°C and then loaded into the sample wells of a 1% agarose gel. After electrophoresis at 100 V for 3 h in 50 mM Tris borate/1 mM EDTA, the gel was stained with ethidium bromide (0.5 μg/ml) for 30 min, destained in water for 60 min, and then photographed over a UV light box.

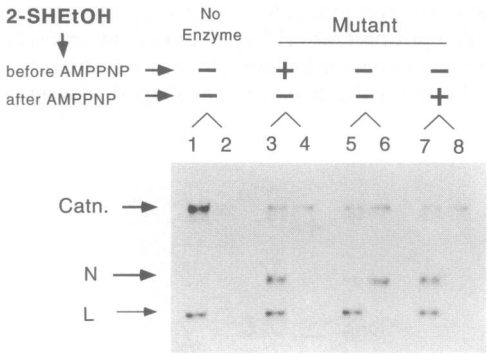

FIG. 5. Single-step decatenation by the N1043C–K1127C mutant yeast DNA topoisomerase II. The DNA substrate was a dimeric catenane composed of an unlabeled supercoiled ring singly linked to a ^{32}P-labeled nicked ring (band Catn.). An appreciable amount of linear DNA was formed during radiolabeling of the nicked ring by nick-translation (band L). Each 50-μl reaction mixture contained 50 mM Tris·HCl (pH 8), 150 mM KCl, 10 mM $MgCl_2$, bovine serum albumin (100 μg/ml), approximately 50 fmol of the dimeric catenane, and 0 or 7 mM 2-mercaptoethanol (2-SHEtOH) as specified by the minus or plus sign, respectively, across the row labeled 2-SHEtOH, before AMPPNP. No enzyme was present in the sample analyzed in lanes 1 and 2, and approximately 50 fmol of the crosslinked N1043C–K1127C mutant enzyme was present in the other reaction mixtures. Single-step decatenation was initiated by the addition of AMPPNP to 2 mM. After 10 min at 30°C, NaCl was added to 1 M. Each sample was filtered through a glass-fiber filter as described (14, 18). DNA samples recovered from the filtrate and the filter were analyzed in the left and right of each pair of adjacent lanes, respectively. Electrophoresis was in 0.8% agarose gel in 50 mM Tris·borate/1 mM EDTA, pH 8.3, and the gel was autoradiographed after drying. Decatenation was evidenced by the appearence of nicked 3-kb DNA ring, the position of which is marked by N in the left margin. Unlabeled 3-kb supercoiled ring resulting from decatenation is invisible in the autoradiogram. For the sample analyzed in the rightmost pair of lanes, 2-mercaptoethanol was added to 7 mM after the addition of NaCl to 1 M.

The result was strikingly different, however, when 2-mercaptoethanol was omitted during incubation of the enzyme–DNA mixture before the addition of AMPPNP. The nicked DNA ring, after its transport through the supercoiled DNA, was not released from the enzyme upon exposure to 1 M NaCl and was found in the filter-retained fraction (Fig. 5, lanes 5 and 6). In control experiments with wild-type yeast DNA topoisomerase II, the unlinked nicked ring was always found in the protein-free fraction whether 2-mercaptoethanol was present or absent during preincubation (data not shown). This experiment provides strong evidence that crosslinking the two enzyme halves across the C-terminal dimer interface prevents exit of the transported DNA.

Further confirmation of the two-gate mechanism was provided by the addition of 2-mercaptoethanol to reduce the disulfide links after the addition of AMPPNP and NaCl. The nicked monomeric DNA ring, which was found in the enzyme-bound fraction before (Fig. 5, lane 6), appeared in the filtrate upon reduction of the disulfide links (Fig. 5, lanes 7 and 8).

The Failure of the Transported DNA Segment to Exit an Enzyme with a Locked C-Terminal Gate Can also Be Demonstrated in the Presence of ATP. To ascertain that the two-gate mechanism, which is strongly supported by the one-step DNA transport experiments described above, was not somehow a special case resulting from the use of a nonhydrolyzable ATP analog, the kinetics of relaxation of supercoiled DNA in the presence of ATP (Fig. 3) was examined in more detail by the use of a single DNA topoisomer. Linking number analysis by two-dimensional agarose gel electrophoresis (27, 28) was employed, so that the linking number changes of the topoisomer products could be followed during incubation with the crosslinked (Fig. 6 *Upper*) or uncrosslinked enzyme (Fig. 6 *Lower*). A mixture of untreated topoisomers served as a calibration for the positions of the various topoisomers. The five other samples examined contained a mixture of the Cys-substituted mutant enzyme and a negatively supercoiled DNA topoisomer with a specific linking number. The samples from left to right were, respectively, incubated in the absence of nucleotides, in the presence of 2 mM AMPPNP, or in the presence of 1 mM ATP for 10 s, 1 min, or 5 min.

For the crosslinked mutant enzyme in the absence of nucleotide (Fig. 6 *Upper*), the linking number *Lk* of the negatively supercoiled DNA topoisomer was not altered by incubation with the enzyme; minor spots representing small amounts of nicked and linear DNA were also present in the untreated sample. Addition of AMPPNP to the enzyme–DNA incubation mixture produced two new topoisomer spots: the major and minor products were formed by a single round of DNA passage by each bound enzyme molecule in DNA rings with one and two bound enzyme molecules per DNA, respectively.

When ATP instead of AMPPNP was added to the reaction mixture containing the crosslinked enzyme, the patterns of DNA topoisomers after incubating the mixture for 10 s, 1 min, or 5 min were nearly identical to those with AMPPNP (Fig. 6 *Upper*). This experiment shows that the C-terminally crosslinked mutant enzyme can efficiently promote a single DNA transport event when AMPPNP or ATP is added, but even in the presence of ATP, the enzyme can not turn over because the T-segment can not escape through the C-gate after its passage through the G-segment.

When 2-mercaptoethanol was added to the incubation mixture, however, the crosslinks were readily disrupted, and the enzyme was shown to catalyze multiple rounds of DNA transport: within 10 s, a fraction of the input negatively supercoiled topoisomer, corresponding in amount to the fraction that showed an *Lk* change of 2 in the absence of 2-mercaptoethanol, was completely relaxed (Fig. 6 *Lower*). These results also showed that under the experimental conditions employed, the enzyme acted processively. While a fraction of DNA molecules, corresponding to those with one or more bound enzyme molecules, was completely relaxed in less than 10 s, the linking number of the bulk of the DNA substrate remained unchanged after 5 min.

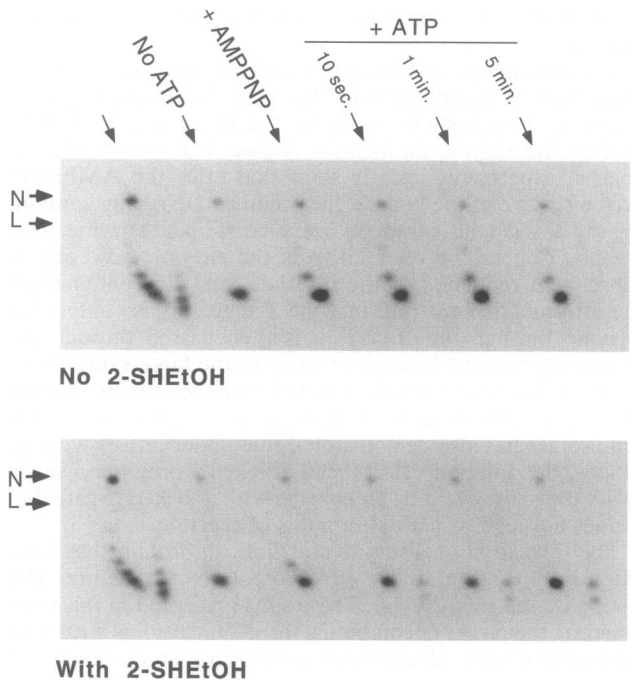

FIG. 6. Analysis of DNA linking number change by the N1043C–K1127C mutant yeast DNA topoisomerase II with and without disulfide crosslinks across the C-gate. Two-dimensional electrophoresis (27, 28) was carried out in 1.2% agarose gel to resolve 2-kb DNA topoisomers of different linking numbers. The electrophoresis buffer was 50 mM Tris·borate, pH 8.3/1 mM EDTA plus chloroquine diphosphate (0.6 μg/ml), in the first dimension (top to bottom), and the same buffer plus chloroquine (3 μg/ml) diphosphate in the second dimension (left to right). Six samples were analyzed in the upper gel shown. The leftmost lane contained a mixture of relaxed and supercoiled topoisomers of different linking numbers to mark their positions in the gel; the mixture also contained nicked circles and trace amount of linear DNA (marked by N and L, respectively). Each of the five samples to the right of the markers contained about 1 nmol of a gel-purified 2-kb topoisomer in 50 μl of 50 mM Tris·HCl, pH 8/150 mM KCl/10 mM $MgCl_2$/bovine serum albumin (100 μg/ml)/ approximately 0.5 nmol of the N1043C–K1127 mutant enzyme. No ATP or AMPPNP was added to the second lane sample, and 2 mM AMPPNP was added to the third lane sample. Samples run in the three rightmost lanes contained 1 mM ATP. After the addition of ATP, these samples were incubated for 10 s, 1 min, and 5 min, respectively, at 30°C and reactions were stopped by the addition of SDS to 1%. The other samples were incubated at 30°C for 5 min before the addition of SDS. Proteinase K was added to the samples to 100 μg/ml and the mixtures were incubated at 60°C for 30 min. A portion of each sample was loaded directly in a sample well of an agarose gel slab for analysis by two-dimensional electrophoresis. Samples analyzed in the lower gel were identical to those analyzed in the corresponding lanes in the upper gel except that the reaction buffer contained 7 mM 2-mercaptoethanol.

DISCUSSION

Based on the recently determined crystal structure of a 92-kDa fragment of yeast DNA topoisomerase II, we were able to design a mutant enzyme with two Cys substitutions such that a pair of disulfide crosslinks can be formed across the C-terminal dimer interface of the enzyme. The formation of these crosslinks is nearly quantitative in the absence of a sulfhydryl reagent and is readily reversed by the addition of 2-mercaptoethanol; these features have allowed us to dissect

the steps after the transport of one DNA double helix through another.

The crosslinked enzyme can efficiently bind and cleave a G-segment in a supercoiled DNA (Fig. 3). As the C-gate is locked in the crosslinked enzyme, the G-segment must have entered the enzyme through the N-gate. The one-step decatenation experiments clearly show that after the AMPPNP-driven closure of the N-gate, the unlinked DNA ring containing the T-segment is trapped in the crosslinked enzyme. This trapped ring can be released from the enzyme, however, by subsequent reduction of the disulfide links. In combination, these results demonstrate that the T-segment also enters the enzyme through the N-gate; it is then passed through the transiently severed G-segment to enter the large central hole in the enzyme and is finally expelled from the enzyme through the C-gate. Relaxation of a negatively supercoiled DNA topoisomer has also demonstrated that under processive conditions, the addition of ATP can efficiently promote a single DNA transport event by an enzyme with a locked C-gate, but it does not lead to multiple rounds of reaction.

The formation of disulfide crosslinks in proteins has been extensively used in studying macromolecular structures (for examples, see refs. 29–34). The results presented in this work illustrate the power of combining three-dimensional structural information with biochemical approaches in mechanistical studies and establish the two-gate mechanism of DNA transport by a type II DNA topoisomerase.

We thank Dr. Janet E. Lindsley for discussions. This work was supported by a grant from National Institutes of Health (GM24544). S.C.H. is an investigator of the Howard Hughes Medical Institute.

1. Gellert, M. (1981) *Annu. Rev. Biochem.* **50,** 879–910.
2. Wang, J. C. (1985) *Annu. Rev. Biochem.* **54,** 665–697.
3. Hsieh, T.-S. (1990) in *DNA Topology and Its Biological Effects*, ed. Cozzarelli, N. R. & Wang, J. C. (Cold Spring Harbor Lab. Press, Plainview, NY), pp. 243–263.
4. Lynn, R., Giaever, G., Swanberg, S. L. & Wang, J. C. (1986) *Science* **233,** 647–649.
5. Uemura, T., Morikawa, K. & Yanagida, M. (1987) *EMBO J.* **6,** 2355–2361.
6. Huang, W. M. (1986) *Nucleic Acids Res.* **14,** 7379–7390.
7. Huang, W. M. (1986) *Nucleic Acids Res.* **14,** 7751–7765.
8. Huang, W. M. (1994) in *DNA Topoisomerases: Biochemistry and Molecular Biology*, ed. Liu, L. F. (Academic, San Diego), pp. 201–225.
9. Wyckoff, E., Natalie, D., Nolan, J. M., Lee, M. & Hsieh, T. (1989) *J. Mol. Biol.* **205,** 1–14.
10. Caron, P. R. & Wang, J. C. (1994) in *DNA Topoisomerases: Biochemistry and Molecular Biology*, ed. Liu, L. F. (Academic, San Diego), pp. 271–297.
11. Yanagida, M. & Sternglanz, R. (1990) in *DNA Topology and Its Biological Effects*, ed. Cozzarelli, N. R. & Wang, J. C. (Cold Spring Harbor Lab. Press, Plainview, NY), pp. 299–320.
12. Ali, J. A., Orphanides, G. & Maxwell, A. (1995) *Biochemistry* **34,** 9801–9808.
13. Wigley, D. B., Davies, G. J., Dodson, E. J., Maxwell, A. & Dodson, G. (1991) *Nature (London)* **351,** 624–629.
14. Roca, J. & Wang, J. C. (1992) *Cell* **71,** 833–840.
15. Mizuuchi, K., Fisher, L. M., O'Dea, M. H. & Gellert, M. (1980) *Proc. Natl. Acad. Sci. USA* **77,** 1847–1851.
16. Wang, J. C., Gumport, R. I., Javaherian, K. J., Kirkegaard, K., Klevan, L., Kotewicz, M. L. & Tse, Y.-C. (1980) in *Mechanistic Studies of DNA Replication and Genetic Recombination*, ed. Alberts, B. (Academic, New York), pp. 769–784.
17. Morrison, A., Brown, P. O., Kruezer, K. N., Otter, R., Gerrard, S. P. & Cozzarelli, N. R. (1980) in *Mechanistic Studies of DNA Replication and Genetic Recombination*, ed. Alberts, B. (Academic, New York), pp. 785–807.
18. Roca, J. & Wang, J. C. (1994) *Cell* **77,** 609–616.
19. Roca, J. & Wang, J. C. (1996) *Genes Cells*, in press.
20. Berger, M. J., Gamblin, S. J., Harrison, S. C. & Wang, J. C. (1996) *Nature (London)* **379,** 225–232.
21. Krasnow, M. A. & Cozzarelli, N. R. (1983) *Cell* **32,** 1313–1324.
22. Giaever, G. N., Snyder, L. & Wang, J. C. (1988) *Biophys. Chem.* **29,** 7–15.
23. Worland, S. T. & Wang, J. C. (1989) *J. Biol. Chem.* **264,** 4412–4416.
24. Jones, T. A., Zou, T. A., Cowan, J. Y. & Kjeldgaard, M. (1991) *Acta Crystallogr. Sect. A* **47,** 110–119.
25. Carson, M. (1991) *J. Appl. Crystallogr.* **24,** 958–961.
26. Liu, L. F. (1989) *Annu. Rev. Biochem.* **58,** 351–375.
27. Lee, C.-H., Mizusawa, H. & Kakefuda, T. (1981) *Proc. Natl. Acad. Sci. USA* **78,** 2838–2842.
28. Wang, J. C., Peck, L. J. & Becherer, K. (1983) *Cold Spring Harbor Symp. Quant. Biol.* **47,** 85–91.
29. Perry, L. J. & Wntzel, R. (1984) *Science* **224,** 555–557.
30. O'Shea, E. K., Rutkowski, R. & Kim, P. S. (1989) *Science* **243,** 538–542.
31. Ewbank, J. J. & Creighton, T. E. (1991) *Nature (London)* **350,** 518–520.
32. Duché, D., Parker, M. W., González-Manas, J.-M., Pattus, F. & Baty, D. (1994) *J. Biol. Chem.* **269,** 6332–6339.
33. Clarke, J., Henrick, K. & Fersht, A. R. (1995) *J. Mol. Biol.* **253,** 493–504.
34. Godley, L, Pfeifer, J., Steinhauer, D., Ely, B., Shaw, G., Kaufman, R., Suchanek, E., Pabo, C., Skehel, J. J., Wiley, D. C. & Worton, S. (1992) *Cell* **68,** 635–645.